



# A stable algorithm for the k-epsilon model for compressible flows

Bijan Mohammadi

## ► To cite this version:

Bijan Mohammadi. A stable algorithm for the k-epsilon model for compressible flows. RR-1355, INRIA. 1990. [inria-00075204](https://hal.inria.fr/inria-00075204)

**HAL Id: [inria-00075204](https://hal.inria.fr/inria-00075204)**

**<https://hal.inria.fr/inria-00075204>**

Submitted on 24 May 2006

**HAL** is a multi-disciplinary open access archive for the deposit and dissemination of scientific research documents, whether they are published or not. The documents may come from teaching and research institutions in France or abroad, or from public or private research centers.

L'archive ouverte pluridisciplinaire **HAL**, est destinée au dépôt et à la diffusion de documents scientifiques de niveau recherche, publiés ou non, émanant des établissements d'enseignement et de recherche français ou étrangers, des laboratoires publics ou privés.

# INRIA

UNITÉ DE RECHERCHE  
INRIA-ROCQUENCOURT

Institut National  
de Recherche  
en Informatique  
et en Automatique

Domaine de Voluceau  
Rocquencourt  
B.P.105  
78153 Le Chesnay Cedex  
France  
Tél.: (1) 39 63 55 11

## Rapports de Recherche

N° 1355

*Programme 7  
Calcul Scientifique,  
Logiciels Numériques et Ingénierie Assistée  
par Ordinateur*

### A STABLE ALGORITHM FOR THE K-EPSILON MODEL FOR COMPRESSIBLE FLOWS

**Bijan MOHAMMADI**

**Décembre 1990**



★ R R . 1 3 5 5 ★

# A STABLE ALGORITHM FOR THE K-EPSILON MODEL FOR COMPRESSIBLE FLOWS

Bijan MOHAMMADI

INRIA-Menusin  
Domaine de Voluceau, 78153 Le Chesnay Cedex, France

## ABSTRACT

*In this work, we report on the performance and difficulties of a  $k, \varepsilon$  model introduced in a Navier-Stokes Finite Volume solver to compute turbulent high speed flows. The equations on turbulent quantities are solved by using a characteristic method for the transport terms and by using a finite element method for the diffusion terms. Furthermore, a new formulation of the  $k, \varepsilon$  model which increases stability is introduced.*

**KEYWORDS :** Turbulence, Navier-Stokes equations, Characteristic method,  $k-\varepsilon$  model, Finite Elements.

## UN ALGORITHME STABLE POUR LE MODELE K-EPSILON POUR LES FLUIDES COMPRESSIBLES.

### RESUME :

*On s'intéresse aux performances ainsi qu'aux difficultés rencontrées lors de l'implémentation d'un modèle  $k, \varepsilon$  dans un solveur volume fini Navier-Stokes pour calculer des écoulements hypersoniques turbulents. Les équations sur les quantités turbulentes sont résolues par la méthode des caractéristiques pour les termes de transport et par une méthode d'éléments finis pour les termes de diffusion. De plus, on propose une nouvelle formulation du modèle  $k, \varepsilon$  qui stabilise le calcul de façon considérable.*

**MOTS-CLES :** Turbulence, équations de Navier-Stokes, méthode des caractéristiques, modèle  $k-\varepsilon$ , éléments finis.

## I. INTRODUCTION

Flows around aircrafts are turbulent, at least in boundary layers and in wakes. This phenomenon has a very great impact on aerodynamic coefficients of industrial interest such as pressure, skin friction and heat transfer coefficients.

Direct simulation of the Navier-Stokes equations and subgrid modeling of the small scales of turbulence in large eddy simulations are useful to improve understanding of turbulence phenomena. However, because of the computer capabilities available (in terms of memory and speed), these methods can not be used nowadays to compute complex configurations. For this reason, statistical turbulence models must be used. We consider here the  $k, \varepsilon$  model developed by Launder and Spalding [LS1]. This is a two equations model, more complex than algebraic models and leads to more numerical problems, also it seems to contain more of the important stress-relaxation properties of the Reynolds stress models (see Coakley [CO1]).

This  $k, \varepsilon$  model was obtained by a generalized of the incompressible model by using Favre averages which preserves the conservative form of the transport equations. Many modifications have been proposed by different authors to take into account more efficiently different compressible effects ; this has led to the introduction of various supplementary terms (see Vandromme [VA1]). Another way to obtain more accurate results in a given flow configuration is to modify the coefficients ( $c_\mu, c_1, c_2$ ) in the  $k, \varepsilon$  equations. The present study is not aimed at a detailed prediction of the flowfield but only at reasonable estimates or trends. We would like however to emphasize numerical problems posed by the implementation of a  $k, \varepsilon$  model in an existing Navier-Stokes solver and to show how it can be done without destroying the stability properties of the solver.

In section II, the Navier-Stokes equations with the  $k, \varepsilon$  model is presented. We also study the turbulence model from the point of view of the numerical analyst and present some results on the positivity and boundedness of  $k$  and  $\varepsilon$ . We then use of these results to propose a new  $(\varphi, \theta)$  model which is more stable than the classical  $k, \varepsilon$  one and which also preserves positivity. A robust numerical method is presented in section III and several numerical examples are given in Section IV.

## II.1. THE NAVIER-STOKES EQUATIONS

Let  $\rho, u, E, p, T, e$  be the density, velocity, total energy, pressure, temperature and internal energy of the fluid. The Navier-Stokes equations are

$$\frac{\partial \rho}{\partial t} + \nabla \cdot (\rho u) = 0 \quad (II.1.1)$$

$$\frac{\partial \rho u}{\partial t} + \nabla \cdot (\rho u \otimes u) = \nabla \cdot \tau \quad (II.1.2)$$

$$\frac{\partial \rho E}{\partial t} + \nabla \cdot (\rho E u) = \nabla \cdot (\tau u) + \nabla \cdot q \quad (II.1.3)$$

with

$$p = (\gamma - 1)\rho e, E = e + \frac{1}{2}u^2, e = C_v T \quad (II.1.4)$$

$$\tau = -pI + \mu\{(\nabla u + \nabla u^T) - \frac{2}{3}(\nabla \cdot u)I\}, q = K\nabla e, K = \mu\frac{\gamma}{Pr} \quad (II.1.5)$$

$$\gamma = C_p/C_v$$

The molecular viscosity  $\mu$ , given by the Sutherland law, is a function of temperature :

$$\mu_{suth} = \mu_\infty \left(\frac{T}{T_\infty}\right)^{1.5} \frac{T_\infty + \frac{110T_\infty}{T}}{T + \frac{110T_\infty}{T}}$$

where  $T_\infty$  and  $\mu_\infty$  are the temperature and the viscosity at infinity.

We denote by  $\langle a \rangle$  the set averaging. This is performed through a large number of records or experiments (for steady solution, this will be the Reynolds average  $\bar{a}$ ). On the other hand, we denote by  $\tilde{a}$  the mass averaging  $\tilde{a} = \langle \rho a \rangle / \langle \rho \rangle$ , and by  $a'$  the fluctuations  $a' = a - \tilde{a}$  of any variable  $a$ . For convenience, we define  $\bar{\rho} = \langle \rho \rangle$ . From (II.1.1)-(II.1.2), we obtain

$$\frac{\partial \bar{\rho}}{\partial t} + \nabla \cdot (\bar{\rho} \tilde{u}) = 0 \quad (II.1.6)$$

$$\frac{\partial \bar{\rho} \tilde{u}}{\partial t} + \nabla \cdot (\bar{\rho} \tilde{u} \otimes \tilde{u}) = \nabla \cdot \langle \tau \rangle - \nabla \cdot \langle \rho u' \otimes u' \rangle \quad (II.1.7)$$

We neglect viscosity fluctuations and we approximate  $\langle \tau \rangle$  by

$$\langle \tau \rangle \equiv -\bar{p}I + \mu\{(\nabla \tilde{u} + \nabla \tilde{u}^T) - \frac{2}{3}(\nabla \cdot \tilde{u})I\}$$

We notice that  $\langle p \rangle = (\gamma - 1)\bar{\rho}\tilde{e} = (\gamma - 1)\bar{\rho}C_v\tilde{T}$ . From (II.1.3), we get

$$\frac{\partial \bar{\rho} \tilde{E}}{\partial t} + \nabla \cdot (\bar{\rho} \tilde{E} \tilde{u}) = -\nabla \cdot \langle \rho E' u' \rangle + \nabla \cdot \langle \tau u \rangle + \nabla \cdot \langle q \rangle \quad (II.1.8)$$

Notice that

$$\tilde{E} = \tilde{e} + \frac{1}{2}(\tilde{u})^2 + \frac{1}{2}(u')^2 \quad (II.1.9)$$

Neglecting third order correlation, we have

$$\langle \rho E' u' \rangle = \langle \rho e' u' \rangle + \langle \rho u' \otimes u' \rangle \tilde{u}$$

Considering the term  $\langle \tau u \rangle$  in (II.1.8), we notice that

$$\langle pu \rangle = (\gamma - 1)\bar{\rho}\tilde{e}\tilde{u} + (\gamma - 1)\langle \rho e' u' \rangle$$

and we assume the approximation

$$\langle \mu \{ (\nabla u + \nabla u^T) - \frac{2}{3}(\nabla \cdot u)I \} u \rangle \equiv \mu \{ (\nabla \tilde{u} + \nabla \tilde{u}^T) - \frac{2}{3}(\nabla \cdot \tilde{u})I \} \tilde{u}$$

The correlation between velocity and temperature fluctuations  $\langle \rho e' u' \rangle$  is modelled by

$$\langle \rho e' u' \rangle = K_t \nabla \tilde{e}, K_t = \mu_t \frac{\gamma}{Pr_t}, Pr_t = 0.9 \quad (II.1.9)$$

As for  $\langle \tau \rangle$ , we neglect thermal conductivity fluctuations and we make the approximation

$$\langle q \rangle = K \nabla \tilde{e}$$

Thus, we obtain the same equation (II.1.1)-(II.1.3) for the average quantities  $\bar{\rho}, \tilde{u}, \tilde{e}$  instead of the instantaneous values  $\rho, u, e$ . But the constitutive relations in (II.1.4), are replaced by

$$p = (\gamma - 1)\bar{\rho}\tilde{e} + \frac{2}{3}\bar{\rho}k, E = \tilde{e} + \frac{1}{2}(\tilde{u})^2 + k, \tilde{e} = C_v \tilde{T} \quad (II.1.10)$$

and in (II.1.5),  $\mu$  and  $K$  are replaced by the total viscosity  $\mu_{total}$  and the total conductivity  $K_{total}$  given by

$$\mu_{total} = \mu + \mu_t, K_{total} = K + K_t \quad (II.1.11)$$

$\mu_t$  and  $K_t$  being defined by (II.2.2) and (II.1.9).

*Remark :*

In all our test cases,  $k$  values appeared to be small compared to the internal energy  $\tilde{e}$ . For this reason, we keep the constitutive relations (II.1.4) instead of (II.1.10). This assumption diminishes the coupling between the averaged flow quantities and the turbulent ones.

## II.2. THE K-EPSILON MODEL

### A) At High Reynolds number

The Reynolds stress tensor  $R$  is given by

$$R = -\frac{2}{3}\rho kI + \mu_t\{(\nabla u + \nabla u^T) - \frac{2}{3}(\nabla \cdot u)I\} \quad (II.2.1)$$

with the turbulent viscosity

$$\mu_t = c_\mu \rho \frac{k^2}{\varepsilon}, c_\mu = 0.09 \quad (II.2.2)$$

It is shown by [CH1] that (II.2.1)-(II.2.2) is quite general in 2D through somewhat restrictive in 3D. As Vandromme [VA1], we consider the following equation for  $k$  where only second order terms have been retained :

$$\frac{\partial \rho k}{\partial t} + \nabla(\rho k u) = Prod + Diff + Diss + Comp$$

where *Prod* represent the production, *Diff* the diffusion, *Diss* the dissipation and *Comp* the main effects of the compressibility on the turbulent kinetic energy :

$$Prod = R : \nabla \tilde{u} = R_{ij} \frac{\partial \tilde{u}_i}{\partial x_j}$$

$$Diff = -\frac{\partial}{\partial x_j} \left( \frac{1}{2} \overline{\rho u'_i u'_j{}^2} + \delta_{ji} \overline{u'_i p'} - \mu \overline{S_{ji} u'_i} \right)$$

$$Diss = -\mu S_{ij} \frac{\partial u'_i}{\partial x_j} \text{ and } Comp = -\tilde{u}'_j \frac{\partial \bar{p}}{\partial x_j} + \overline{p' \frac{\partial u'_j}{\partial x_j}}$$

where  $S$  is the deformation tensor.  $S = \nabla \tilde{u} + \nabla \tilde{u}^t - \frac{2}{3} \nabla \cdot \tilde{u}$ .

We model the unknown correlations in the previous equation as follows :

The turbulent diffusion is supposed to have the same structure as the viscous one for high Reynolds number flow, so if we denote by  $\sigma_k$  the turbulent Prandtl-Schmidt number of  $k$ , we can write :

$$Diff = \nabla \cdot \left( \frac{\mu_t}{\sigma_k} \nabla k \right)$$

The pressure dilatation effect can be modelled following Grasso [GRA1] :

$$Comp = \left( \frac{c_k \bar{p}}{\bar{p}} \right) \mu_t (\tilde{u} \cdot R \cdot \tilde{u}) \nabla \cdot \tilde{u}$$

This model is obtained under hypothesis that the flow is statically steady. Hence, the model can only be used for such a flow. Furthermore, the explicit dependence on the mean velocity  $\bar{u}$  in this model make it clearly no galilean invariant. In addition, new terms can be introduced to take into account the variation of the density (see [VA1], [JO1]) for multi component fluids with or without combustion. All of these terms introduce new constants which must be numerically tuned. For these reasons, we will not take into account the compressible effects *Comp* in the numerical application. Finally, we define the turbulent dissipation by :

$$\bar{\rho}\varepsilon = \overline{\mu S : \nabla u'}$$

Hence, the  $k$  equation can be rewritten as :

$$\frac{\partial \bar{\rho}k}{\partial t} + \nabla(\bar{\rho}\bar{u}k) - \nabla\left(\frac{\mu_t}{\sigma_k}\nabla k\right) = R : \nabla\bar{u} - \bar{\rho}\varepsilon + \frac{c_k\bar{\rho}}{\bar{p}}(\bar{u}R\bar{u})\nabla \cdot \bar{u}$$

For the transport equation on  $\varepsilon$  we make the hypothesis that there is analogy between the  $k$  and the  $\varepsilon$  equations in high Reynolds number situations.

Hence, the differences are on rates and on time scales ; we consider the following  $\varepsilon$  equation :

$$\frac{\partial \bar{\rho}\varepsilon}{\partial t} + \nabla(\bar{\rho}\bar{u}\varepsilon) - \nabla\left(\frac{\mu_t}{\sigma_\varepsilon}\nabla\varepsilon\right) = \frac{\varepsilon}{k}(c_{1\varepsilon}R : \nabla\bar{u} - c_{2\varepsilon}\bar{\rho}\varepsilon + c_{3\varepsilon}c_k\frac{\bar{\rho}}{\bar{p}}\mu_t(\bar{u}R\bar{u})\nabla \cdot \bar{u})$$

## B) Near Wall Region

The previous model has been established under the hypothesis that the Reynolds number is high ; so we cannot consider regions close to a solid wall where the Reynolds number decreases.

The most widely used approach when dealing with the near wall regions difficulties is to avoid solving the NS equations (including the turbulence model) right up to the wall. Instead, the edge of the computational domain is placed a small distance  $\delta$  away from the wall in the high Reynolds number region (fully developed turbulent region). Empirical laws are then used to define boundary conditions at the edge of the domain (the subscript  $w$  and  $\delta$  would mean at the wall and at the artificial wall boundary).

The friction velocity  $u_\tau = \frac{\tau}{\rho}$  is evaluated from  $u_\tau = \frac{u}{y^+}$ , if  $y^+ \leq 10$  and from  $u_\tau = U_c / (\frac{1}{\kappa} \log(y^+) + \beta)$  where  $\kappa = .41, \beta = 5.5$  if  $y^+ \geq 10$ .  $U_c = \int_0^{u^*} \frac{\rho \varepsilon}{\rho_w} du$  is the van Driest compressibility transformation. Once  $u_\tau$  is computed, the boundary conditions on the computational domain on  $k$  and  $\varepsilon$  are :

$$k_\delta = \frac{u_\tau^2}{\sqrt{c_\mu}} \frac{\rho_w}{\rho_\delta}, \varepsilon_\delta = \frac{u_\tau^3}{\kappa \delta} \left(\frac{\rho_w}{\rho_\delta}\right)^{\frac{3}{2}} \quad (II.2.B.1)$$



If we denote  $N = (\mu + \mu_t)(\nabla u + \nabla u^t - \frac{2}{3}\nabla \cdot u)$  the viscous part of the stress tensor,  $\vec{\tau}$  a unit vector tangential to  $\Gamma$  and  $\vec{n}$  the unit outward normal to  $\Gamma$ , the boundary conditions on the NS variables are :

$$\vec{u} \cdot \vec{n} = 0$$

$$\vec{\tau} \cdot N \cdot \vec{n} = -\rho u_\tau^2$$

$$\vec{u} \cdot N \cdot \vec{n} + (\kappa + \kappa_t) \frac{\partial T}{\partial n} = -\rho u_\tau^2 \tau (\vec{u} \cdot \vec{\tau}) + T_\tau u_\tau$$

where  $T_\tau$  is the friction temperature defined by :

$$u_\tau T_\tau = (\kappa + \kappa_t) \nabla T \cdot n$$

The temperature profile is taken to be similar to the velocity one, therefore  $T_\tau$  is evaluated (see [BR1]) as  $T_\tau = \frac{T_w - T_\infty}{Pr y^+}$  if  $y^+ \leq 16$  and  $T_\tau = \frac{T_w - T_\infty}{\frac{1}{\kappa} \log(y^+) + c}$  if  $y^+ \geq 16$ . For a cold wall we take  $Pr = .71, \kappa = .41$  and  $c = 2$ . (see Cheng and Ng [CH1]). In appendix B we check a few necessary conditions for the suitability of the NS equations with such a slip boundary conditions.

In the previous set of wall laws, the friction velocity is defined only from the mean flow, it seems to be interesting to reduce this close connection by introducing a more fundamental velocity scale :  $\sqrt{k}$ , dedicated to describing turbulent quantities. Indeed, if the computational domain boundary is placed at a distance  $\delta$ , to the wall, in the fully turbulent region where we assume to have equilibrium between production and dissipation of the turbulent kinetic energy ( $y$  is the normal direction) :

$$-\overline{\rho u'v'} \frac{\partial \bar{u}}{\partial y} = \bar{\rho} \varepsilon$$

now, we introduce  $u_\tau^k = c_\mu^{\frac{1}{4}} k^{\frac{1}{2}}$  and  $u_\tau^l = \frac{\bar{u} \cdot \vec{\tau}}{(1/\kappa) \log(y^+) + \beta}$  two friction velocities such that  $-\overline{\rho u'v'} = \bar{\rho}_w u_\tau^{k2}$  and  $\frac{\partial \bar{u}}{\partial y} = u_\tau^l / \kappa \delta$ . The boundary condition on  $\varepsilon$  is then

$$\varepsilon = \left(\frac{\rho_w}{\rho \delta}\right)^{\frac{3}{2}} (u_\tau^{k2} u_\tau^l / \kappa \delta)$$

This approach improves the prediction of the turbulent quantities in the regions where the friction to the wall decreases but where the turbulence has still high level.

### II.3. NUMERICAL BEHAVIOUR OF $k$ AND EPSILON

Now, in order to simplify the writing, the average quantities  $\bar{\rho}$ ,  $\bar{u}$ ,  $\bar{\epsilon}$  will be denoted without bar or tilde.

We consider the non conservative form of the  $k - \epsilon$  model which contains the main source of instabilities :

$$\frac{\partial k}{\partial t} + u \cdot \nabla k - \frac{1}{\rho} \nabla \cdot \left( \left( \mu + \frac{\mu_t}{\sigma_k} \right) \nabla k \right) = c_\mu \frac{k^2}{\epsilon} F - \frac{2}{3} k \nabla \cdot u - \epsilon \quad (II.3.1)$$

$$\frac{\partial \epsilon}{\partial t} + u \cdot \nabla \epsilon - \frac{1}{\rho} \nabla \cdot \left( \left( \mu + \frac{\mu_t}{\sigma_\epsilon} \right) \nabla \epsilon \right) = c_1 k F - \frac{2c_1}{3c_\mu} \epsilon \nabla \cdot u - c_2 \frac{\epsilon^2}{k} \quad (II.3.2)$$

$$c_1 = 0.1296, c_2 = 1.92, c_\mu = 0.09, \sigma_k = 1, \sigma_\epsilon = 1.3$$

where  $F = \frac{1}{2} |\nabla u + \nabla u^T|^2 - \frac{2}{3} (\nabla \cdot u)^2 \leq 0$  and  $\nabla \cdot u$ . The  $k$  and  $\epsilon$  equations show that the compression and expansion produce the same effects in both of them ; indeed, compression ( $\frac{-2}{3} k D \leq 0$ ) tends to increase turbulence, while expansion does the reverse, this is in agreement with the experimental results of Wu et al [WU1]. In [Ah1], we can find several additional terms for the  $\epsilon$  equation to take into account other compressibility effects, but it is not clear that the model is better with these new terms.

#### Positivity of $k$ and $\epsilon$

For physical reasons, it is important that the  $k - \epsilon$  model guaranties the positivity of  $k$  and  $\epsilon$  if they are positive initially. For this purpose, we suppose that the system has a smooth solution for given positive data and we introduce a new variable  $\theta = \frac{k}{\epsilon}$  (the turbulent time scale) as in Cardot [Ca1], the  $\theta$  equation can be obtained from the  $k$  and  $\epsilon$  one, as follows (we denote by  $\frac{d}{dt}$  the convective derivative) :

$$\frac{d\theta}{dt} = \frac{\partial \theta}{\partial t} + u \cdot \nabla \theta = \frac{1}{\epsilon} \frac{dk}{dt} - \frac{k}{\epsilon^2} \frac{d\epsilon}{dt} = -a\theta^2 + b\theta + c + Diff$$

where  $a = (c_1 - c_\mu)F$ ,  $b = \frac{2}{3} \left( \frac{c_1}{c_\mu} - 1 \right) D$  and  $c = c_2 - 1$ ; Diff is the contribution of the viscous terms of the  $k$  and  $\epsilon$  equations :

$$Diff = \left( \frac{c_\mu}{\sigma_k} + \frac{2c_\mu}{\sigma_\epsilon} \right) \theta \nabla k \nabla \theta + \left( \frac{c_\mu}{\sigma_k} - \frac{c_\mu}{\sigma_\epsilon} \right) (\theta^2 \Delta k + \frac{\theta^2}{k} |\nabla k|^2) \\ + \left( \frac{c_\mu}{\sigma_k} - \frac{c_\mu}{\sigma_\epsilon} \right) \frac{\theta^2}{\rho} \nabla \rho \nabla k + \frac{c_\mu}{\sigma_\epsilon} \frac{k\theta}{\rho} \nabla \theta \nabla \rho$$

So the compressibility has an inverse effect on  $\theta$  compared to  $k$  and  $\varepsilon$ .

Now, through the  $\theta$  equation, one can prove

**Theorem:**  $k$  and  $\varepsilon$  stay positive if they are positive initially and if  $\sigma_k = \sigma_\varepsilon$ .

*proof:* Because  $c_\mu \geq c_1$  and  $c_2 \leq 1$ ,  $\theta$  will stay positive and bounded when there are no diffusion terms ; indeed if  $F$  and  $D$  are taken constant on the characteristics curves. The dynamical part of the  $\theta$  equation:

$$\frac{d\theta}{dt} = -aF\theta^2 + bD\theta + c \quad (T)$$

with

$$\theta(0) = \frac{k(0)}{\varepsilon(0)} = \theta_0$$

is a Riccati equation, after integration in time we have :

$$\theta(t) = \frac{\theta_1 - K\theta_2 e^{-s}}{1 - K e^{-s}} \quad (II.3.4)$$

where  $s = ((bD)^2 + 4acF)^{\frac{1}{2}} t \leq 0$ ,  $K = (\theta_0 - \theta_2)/(\theta_0 - \theta_1)$  and  $\theta_{1,2}$  roots of the RHS of (T). Hence, if  $\theta$  is initially positive, it stays positive and bounded (see [Ca1] for the proof for incompressible fluids). On the other hand,  $\theta$  cannot become negative in the presence of the viscous terms *Diff*. Call  $t$  the first time there exists  $x$  such that  $\theta(x, t) = 0$  ; because we have positive boundary and initial conditions for  $\theta$ ,  $x$  is strictly inside  $\Omega \times ]0, T[$  and so at this point we must have  $\nabla\theta = 0$  (it is a minimum).

Hence  $\frac{d\theta}{dt} = c_2 - 1 > 0$  so  $\theta$  increases again.

Furthermore, introducing  $\theta$  in the  $k$  and  $\varepsilon$  equations, we have

$$\begin{aligned} \frac{\partial k}{\partial t} + u \cdot \nabla k - \frac{1}{\rho} \nabla \cdot \left( \left( \mu + \frac{c_\mu \rho k \theta}{\sigma_k} \right) \nabla k \right) &= c_\mu k \theta F - \frac{2}{3} k \nabla \cdot u - \frac{k}{\theta} \\ \frac{\partial \varepsilon}{\partial t} + u \cdot \nabla \varepsilon - \frac{1}{\rho} \nabla \cdot \left( \left( \mu + \frac{c_\mu \rho k \theta}{\sigma_\varepsilon} \right) \nabla \varepsilon \right) &= c_1 \varepsilon \theta F - \frac{2c_1}{3c_\mu} \varepsilon \nabla \cdot u - c_2 \frac{\varepsilon}{\theta} \end{aligned}$$

Denote by  $(x_m, t_m)$  the point at which  $k$  (resp.  $\varepsilon$ ) is minimum. Suppose this minimum is 0. When positive Dirichlet boundary condition are added to these equations,  $x_m$  cannot be on the boundary. So at  $(x_m, t_m)$  we will have  $k = 0$  and  $\nabla k = 0$  (resp.  $\varepsilon = 0$  and  $\nabla \varepsilon = 0$ ). But, we have shown that  $\theta$  is always positive at  $(x_m, t_m)$  so we have

$$\frac{\partial k}{\partial t} = 0 \text{ resp. } \frac{\partial \varepsilon}{\partial t} = 0$$

Thus  $k$  (resp.  $\varepsilon$ ) becomes stationary and never negative.

Such an argument proves that the coupled system  $(k - \varepsilon)$ , and not each equation individually, has a positive solution.

### *Stability of the $k, \varepsilon$ system*

Another major difficulty, if we have to use the  $(k - \varepsilon)$  model, is that there is the possibility of an exponential blow up for  $k$  and  $\varepsilon$ . Indeed, if  $s \rightarrow \infty$  in (II.3.4),  $\theta \rightarrow \theta_1$  a constant and the  $k$  and  $\varepsilon$  equations are then

$$\frac{dk}{dt} = k\left(\theta_1 F - \frac{2}{3}D - \frac{1}{\theta_1}\right)$$

$$\frac{d\varepsilon}{dt} = \varepsilon\left(\theta_1 F - \frac{2}{3}D - \frac{1}{\theta_1}\right)$$

Therefore, if  $F$  is sufficiently large, both of  $k$  and  $\varepsilon$  grow exponentially.

As shown,  $\theta = \frac{k}{\varepsilon}$  has a good numerical behaviour (bounded and positive), the idea is then to find another combination  $\varphi$  of  $k$  and  $\varepsilon$ , that is dynamically stable ( $\frac{d\varphi}{dt} \geq 0$ ). Because of the similar behaviour of  $k$  and  $\varepsilon$ , we look at the dynamical part of their equations and try to find  $\varphi = k^\alpha \varepsilon^\beta$  with  $\alpha$  and  $\beta$  real.

The  $\varphi$  equation comes from those of  $k$  and  $\varepsilon$  as for  $\theta$  (without viscous terms):

$$\frac{d\varphi}{dt} = k^\alpha \varepsilon^\beta (aFk + bD + c\frac{\varepsilon}{k}) \quad (\phi)$$

where  $a = \alpha c_\mu + \beta c_1$ ,  $b = -\alpha - c_1 \beta / c_\mu$  and  $c = -\alpha - \beta c_2$ .

$\varphi$  will decrease ( $\frac{d\varphi}{dt} \leq 0$ ) if  $a, b$  and  $c$  are negative ; furthermore,  $\frac{c_1}{c_\mu} < c_2$  implies that  $\beta > 0$  and  $a > 0, b > 0$  imply  $\alpha c_\mu + \beta c_1 = 0$ . One possibility is then  $\alpha = -c_1 / c_\mu$  and  $\beta = 1$  and we have

$$\frac{d\varphi}{dt} = -(c_2 - \frac{c_1}{c_\mu}) \frac{\varphi}{\theta} \leq 0$$

Notice that there is no mean flow terms in this equation and that the coupling between  $\theta$  and  $\varphi$  is weaker than in the original  $k - \varepsilon$  model. But viscous terms must still be added.

Of course other choices of  $\varphi$  are possible by studying the coupled system  $(T, \phi)$ . In [CA2] one gives a few tools for the implementation of such a model.

*Remark*

We can make a similar analysis for the low Reynolds number versions of the  $k, \varepsilon$  model; in these models, the constants  $(c_\mu, c_1, c_2)$  are multiplied by positive functions  $(f_\mu, f_1, f_2)$  which depend on  $R_y = \rho k^2 / \mu \varepsilon$  and  $R_t = \rho \sqrt{k} y / \mu$  two local Reynolds numbers [Pal]. Hence, in  $\phi$ , we have now  $a = \alpha c_\mu f_\mu + \beta c_1 f_1$ ,  $b = -\alpha - c_1 f_1 \beta / c_\mu$  and  $c = -\alpha - \beta f_2 c_2$ . Because  $0 < f_\mu \leq 1$ ,  $\beta$  must be negative and if we take  $\alpha = f_1 c_1 / c_\mu$  we have

$$\frac{d\varphi}{dt} = (c_2 f_2 - \frac{c_1 f_1}{c_\mu}) \frac{\varphi}{\theta}$$

So for  $\varphi$  to decrease, we must have  $f_2 \leq \frac{c_1 f_1}{c_2 c_\mu}$ ; but this is only partially true because  $1 \geq f_1$  and  $0 < f_2 \leq 1$ . This is not really surprising because  $k, \varepsilon$  and  $u$  have very stiff profiles in the near wall regions. On the other hand, the low Reynolds number  $\theta$  equation is :

$$\frac{d\theta}{dt} + Diff = -aF\theta^2 + bD\theta + f_2 c_2 - 1.$$

Hence, this version of the  $\theta$  equation is more stable than the high Reynolds number version ( $a = f_1 c_1 - f_\mu c_\mu \leq c_1 - c_\mu$ ).

*A new  $\varphi, \theta$  turbulence model*

As it shown, the introduction of the  $\varphi, \theta$  variables avoids the main difficulties of the  $k, \varepsilon$  model. So it is interesting to find two diffusion constants for  $\varphi$  and  $\theta$  and to solve then completely the  $\varphi, \theta$  equations. On the other hand, theoretical results are available for the  $\varphi, \theta$  model. In [LE1] we give some results on the existence and regularity of the solutions of this model for incompressible flows.

Cardot has presented an incompressible  $k - \theta$  version of the  $k, \varepsilon$  model which is numerically more stable. The constants in the  $\theta$  equation are obtained from the  $k - \varepsilon$  one for the dynamical part and the viscous constant  $\sigma_\theta = 0.1$  is numerically tuned for the Poiseuille flow. If we follow the same approach the  $\theta$  equation would be :

$$\frac{d\theta}{dt} - \frac{1}{\rho} \nabla \cdot (\frac{c_\mu}{\sigma_\theta} k \theta \nabla \theta) = -(c_1 - c_\mu) F \theta^2 + \frac{2}{3} (\frac{c_1}{c_\mu} - 1) D \theta + c_2 - 1.$$

### III. THE COMPUTATIONAL METHOD

In order to solve the partial differential equations on  $\rho, u, e, k, \varepsilon$  we first make a splitting.

With  $k, \varepsilon$  known at time step  $t^n$ , we evaluate the turbulent viscosity and thermal conductivity by (II.2.2) and (II.1.9) then we solve the Navier-Stokes equations (II.1.1)-(II.1.3) on  $[t^n, t^{n+1}]$  with viscosity and conductivity given by (II.14). This gives  $\rho^{n+1}, u^{n+1}, e^{n+1}$ . We then solve the equations (II.3.1), (II.3.2) in order to get  $k^{n+1}, \varepsilon^{n+1}$  and we iterate on  $n$ .

The Navier-Stokes solver was developed by Rostand and Stoufflet [RO1]. It is derived from an implicit algorithm for solving Euler equations on unstructured triangular grids and is based on a finite-volume approximation of the equations in conservation form, using control volumes defined by the medians of the triangle surrounding each node and Osher's flux formula for the convective part and a centred scheme for the diffusive one (see appendix A).

#### 1) Computation of $k$ and $\varepsilon$

Because of the splitting mentioned, to solve  $k, \varepsilon$  equations, we assume that  $\rho, u, T$  are given and constant during the time step  $[t^n, t^{n+1}]$ . To compute  $k$  and  $\varepsilon$ , we then make another splitting between the transport terms and the diffusion terms in equations (II.15), (II.16).

##### a) The transport step

Without the diffusion terms, (II.15), (II.16) are

$$\frac{\partial k}{\partial t} + u \cdot \nabla k = S_k = \frac{c_\mu}{2} \frac{k^2}{\varepsilon} |\nabla u + \nabla u^T|^2 - \varepsilon - \frac{2}{3} (k + c_\mu \frac{k^2}{\varepsilon} \nabla \cdot u) \nabla \cdot u \quad (III.1)$$

$$\frac{\partial \varepsilon}{\partial t} + u \cdot \nabla \varepsilon = S_\varepsilon = c_1 k |\nabla u + \nabla u^T|^2 - c_2 \frac{\varepsilon^2}{k} - \frac{2c_1}{3} (\frac{\varepsilon}{c_\mu} + k \nabla \cdot u) \nabla \cdot u \quad (III.2)$$

These equations are solved using a method of characteristics ([BE1], [Pi1]), we retain the idea of Benqué et al to integrate the source terms on the characteristics because for a fixed time step the source terms have large variations on the travel path  $[x, X^n(x)]$ . Furthermore, the method preserves the positivity of  $k$  and  $\varepsilon$  if they are positive initially.

So we consider the characteristic issued from  $x$

$$\frac{d}{d\tau} X^n(\tau) = u(\tau, X^n(\tau)), X^n(t^{n+1}) = x, \quad \tau \in [t^n, t^{n+1}] \quad (III.3)$$

and decompose the source term in the following way

$$S_k = S_k^+ - S_k^- k, S_k^+ = c_\mu \frac{k^2}{\varepsilon} F, S_k^- = \frac{\varepsilon}{k} \quad (III.4)$$

where  $F = \frac{1}{2}|\nabla u + \nabla u^t|^2 - \frac{2}{3}(\nabla \cdot u)^2 \leq 0$ . The position (right or left hand side) of the other term  $\frac{2}{3}k\nabla \cdot u$  depends on the sign of  $\nabla \cdot u$ . Then,  $S_k^+$  and  $S_k^-$  are both positive. Both of them are treated explicitly, the values for  $k$  and  $\varepsilon$  being those at the beginning of the time step,  $k^n, \varepsilon^n$ . After integration along the characteristic, we find at  $t^{n+1}$  the value of  $k$  (resp.  $\varepsilon$ ), which we denote by  $k^{n+\frac{1}{2}}$  (resp.  $\varepsilon^{n+\frac{1}{2}}$ ) such that

$$\begin{aligned} & (1 + \int_{t^n}^{t^{n+1}} S_k^-(X^n(\tau))d\tau)k^{n+\frac{1}{2}}(x) \\ &= k^n \circ X^n(t^n) + (\int_{t^n}^{t^{n+1}} S_k^+(X^n(\tau))d\tau) \end{aligned} \quad (III.5)$$

$$\begin{aligned} & (1 + \int_{t^n}^{t^{n+1}} S_\varepsilon^-(X^n(\tau))d\tau)\varepsilon^{n+\frac{1}{2}}(x) \\ &= \varepsilon^n \circ X^n(t^n) + (\int_{t^n}^{t^{n+1}} S_\varepsilon^+(X^n(\tau))d\tau) \end{aligned} \quad (III.5.bis)$$

This treatment of the source terms (explicit for the positive part and semi-implicit for the negative part) tempers the exponential growth of  $k$  and  $\varepsilon$  when  $F$  is large and the decay of the same quantities when  $F$  is small.

Furthermore, if we completely semi-implicit  $S_k$  and  $S_\varepsilon$ , we obtain two stability conditions for the time step  $\Delta t = t^{n+1} - t^n$ . Indeed, for  $k$  and  $\varepsilon$  to stay positive we must have  $\Delta t$  such that

$$\int_{t^n}^{t^{n+1}} (S_k^- - \frac{S_k^+}{k})(X^n(\tau))d\tau > -1$$

and

$$\int_{t^n}^{t^{n+1}} (S_\varepsilon^- - \frac{S_\varepsilon^+}{\varepsilon})(X^n(\tau))d\tau > -1$$

Hence, one reduces the time step when the production is more important than the dissipation. Notice that the characteristics are only computed one for each node and that we integrate four different quantities ( $S_k^+, S_k^-, S_\varepsilon^+, S_\varepsilon^-$ ) along these characteristics using trapezoidal method.

This approach guaranties the positivity of  $k$  and  $\varepsilon$ , but despite the time step restriction mentioned before, it does not prevent the possibility of a blow up for  $k$  and  $\varepsilon$ . To improve the robustness and stability of the method, we introduce  $\theta$  and

$\varphi$  as presented in II. Thus, knowing  $k^n$  and  $\varepsilon^n$ , we evaluate  $\varphi^n = k^{n-\frac{c_1}{c_\mu}} \varepsilon^n$  and  $\theta^n = \frac{k^n}{\varepsilon^n}$ . Now, using the integration along the characteristics as above, we have :

$$(1 + \int_{t^n}^{t^{n+1}} S_\varphi^-(X^n(\tau))d\tau)\varphi^{n+\frac{1}{2}}(x) = \varphi^n \circ X^n(t^n)$$

$$\begin{aligned} & (1 + \int_{t^n}^{t^{n+1}} S_\theta^-(X^n(\tau))d\tau)\theta^{n+\frac{1}{2}}(x) \\ &= \theta^n \circ X^n(t^n) + \int_{t^n}^{t^{n+1}} S_\theta^+(X^n(\tau))d\tau \end{aligned}$$

Finally,

$$k^{n+\frac{1}{2}} = (\theta^{n+\frac{1}{2}}\varphi^{n+\frac{1}{2}})^{\frac{c_\mu}{c_\mu-c_1}} \quad \text{and} \quad \varepsilon^{n+\frac{1}{2}} = \theta^{n+\frac{1}{2}}\varphi^{n+\frac{1}{2}}\varphi^{n+\frac{1}{2}}^{\frac{c_\mu}{c_\mu-c_1}}$$

Hence, because we know that  $\varphi$  and  $\theta$  stay bounded and positive, the algorithm will be robust.

Furthermore, in the incompressible case, the previous scheme is second order accurate for  $\theta$  ; indeed, consider the following initial value problem :

$$\frac{d\theta}{dt} = S(\theta), \quad \theta(0) = \theta_0 \quad (E1)$$

Then

$$\theta(\Delta t) = \theta_0 + \Delta t S(\theta_0) + \frac{(\Delta t)^2}{2} S(\theta_0)S'(\theta_0) + 0(\Delta t^2)$$

If

$$S(\theta_0) = R(\theta_0) = L(\theta_0)\theta_0$$

then

$$\theta(t) = \frac{\theta_0 + \Delta t R(\theta_0)}{1 + \Delta t L(\theta_0)} = \frac{\theta_0 + \Delta t (S(\theta_0) + \theta_0 L(\theta_0))}{1 + \Delta t L(\theta_0)}$$

$$= \theta_0 + \Delta t S(\theta_0) + \Delta t^2 (L^2(\theta_0)\theta_0 - (S(\theta_0) + \theta_0 L(\theta_0))L(\theta_0)) + 0(\Delta t^2)$$

Hence, to have second order accuracy, we must have  $L(\theta_0) = -\frac{1}{2}S'(\theta_0)$  ; but  $S_\theta = -a\theta^2 + c$  and  $L(\theta_0) = -a\theta_0$ . In the compressible situation, the scheme stays second order accurate for  $\theta$  is we have only dilatation ( $\nabla \cdot u \geq 0$ ).

b) *The diffusion step*

To obtain  $k^{n+1}, \varepsilon^{n+1}$ , we solve

$$\frac{\partial k}{\partial t} = \nabla \cdot \left( \left( \mu + \frac{\mu_t}{\sigma_k} \right) \nabla k \right) \quad (III.6)$$



$$\frac{\partial \varepsilon}{\partial t} = \nabla \cdot \left( \left( \mu + \frac{\mu_t}{\sigma_\varepsilon} \right) \nabla \varepsilon \right) \quad (III.7)$$

on  $[t^n, t^{n+1}]$  starting from the value obtained at the end of the transport resolution  $k^{n+\frac{1}{2}}, \varepsilon^{n+\frac{1}{2}}$ . The viscosities in (III.6), (III.7),  $\mu + (\mu_t/\sigma_k)$  and  $\mu + (\mu_t/\sigma_\varepsilon)$  are evaluated explicitly. Diffusion is then solved implicitly using a standard finite element method with a  $P1$  continuous discretization of  $k$  and  $\varepsilon$  on the triangles. However, in order to preserve positivity, it is necessary to use mass-lumping (see Zienkiewics [ZI1]). Positivity of the overall algorithm is then obtained (strictly provided there is not obtuse angle in the mesh) with no condition on the time step. For easy vectorisation, the linear system obtained with this finite element method is solved using Jacobi's method.

## 2) Boundary conditions on $k$ and $\varepsilon$

The equations (II.3.1), (II.3.2) are supplemented with the following boundary conditions.

At infinity, values for  $k$  and  $\varepsilon$  are prescribed

$$k = k_\infty, \quad \varepsilon = \varepsilon_\infty \quad (III.8)$$

On wall boundaries, the natural boundary conditions are of course

$$k = 0, \quad \varepsilon = \varepsilon_w, \quad u = 0 \quad (III.9)$$

But usually, wall laws are used, this makes possible to have less grid points near the wall. For the time being, we use one of the two set of wall laws mentioned in (II.2.B) at the boundary of the computational domain ( $\delta$ -wall) which is at a distance  $\delta$  from the solid wall.

### *Numerical treatment of the boundary conditions*

- For the resolution of the transport equations, we have to prescribe the value of  $k$  and  $\varepsilon$  at the boundary when  $u \cdot n < 0$  ( $n$  being the outward normal to the computational domain). Therefore no boundary conditions are needed at the wall nor at outflow boundaries for this transport phase.

- For the diffusion equations, we take the Neumann condition at infinity and the Dirichlet one at the wall.

- We take into account the boundary conditions on the NS quantities through the viscous part of the boundary integrals which appear in the finite volume Galerkin formulation of the NS equations. Indeed, if  $n$  is the outward normal and  $N = (\mu + \mu_t)(\nabla \cdot u + \nabla \cdot u^t - \frac{2}{3} \nabla \cdot u I)$  the viscous part of the stress tensor,

using divergence formula, the viscous contributions on the boundaries are, for the momentum equation :

$$\int_{\Omega} \nabla \cdot (N) dx = \int_{\Gamma} N \cdot n d\sigma = \int_{\Gamma_w \cup \Gamma_{\infty}} N \cdot n d\sigma$$

We suppose that  $N$  vanishes at infinity and that the tangential variation of the velocity is negligible compared to the normal one (i.e.  $n \cdot N \cdot n \ll \tau \cdot N \cdot n$ ) ; now using the definition of the friction velocity ( $-\rho u_{\tau}^2 = \tau \cdot N \cdot n$ ) we have :

$$\int_{\Gamma_w} (\tau \cdot N \cdot n) \tau d\sigma = \int_{\Gamma_w} -\rho u_{\tau}^2 d\sigma$$

The same reasons imply that for the energy equation, using divergence formula, we have :

$$\begin{aligned} \int_{\Omega} \nabla \cdot (N \cdot u + q) dx &= \int_{\Gamma} (u \cdot N \cdot n + q \cdot n) d\sigma = \int_{\Gamma_w} (u \cdot N \cdot n + q \cdot n) d\sigma \\ &= \int_{\Gamma_w} ((-\rho u \cdot \tau) u_{\tau}^2 + u_{\tau} T_{\tau}) d\sigma \end{aligned}$$

where  $T_{\tau}$  is the friction temperature defined by :

$$u_{\tau} T_{\tau} = (\kappa + \kappa_t) \nabla T \cdot n$$

$T_{\tau}$  is evaluated thanks to (II.2.B).

- Because of the linearized implicit scheme we use in the NS solver, the previous friction boundary conditions come into the matrix of the system. Indeed, we have  $-\rho u_{\tau}^2 = II = -\rho(\vec{u} \cdot \vec{\tau})^2 / u^{+2}$  where  $u^{+}$  is a given function of  $\delta^{+} = \rho \delta u_{\tau} / \mu$  (see II.2.B) ; we then take semi-implicit the upper part of the right hand side of II

$$II = -(\rho^{n+1} u^{\overline{n+1}} \cdot \vec{\tau}) / (u^{+n})^2$$

and we linearize this expression with respect to conservative variables.

## VI. DISCUSSION OF THE RESULTS

Several results are presented for three test cases. To show the impact of the  $\varphi - \theta$  model on the stability of the method, we are particularly interested in the convergence history of  $k$  and  $\varepsilon$ .

### *Grid turbulence*

For this test case, an analytical solution of the  $k, \varepsilon$  equations is available. Indeed, one consider a constant velocity field  $u = 1, v = 0$  which convect an homogenous turbulence  $k = k_0, \varepsilon = \varepsilon_0$ . The viscous and the production effects are negligible and the system is reduced to ( $x$  being the convective direction) :

$$k_{,x} = -\varepsilon, \varepsilon_{,x} = -\frac{\varepsilon^2}{k}$$

$$k(0) = k_0, \varepsilon(0) = \varepsilon_0$$

Now introducing  $\theta = k/\varepsilon$ , we have the following solutions

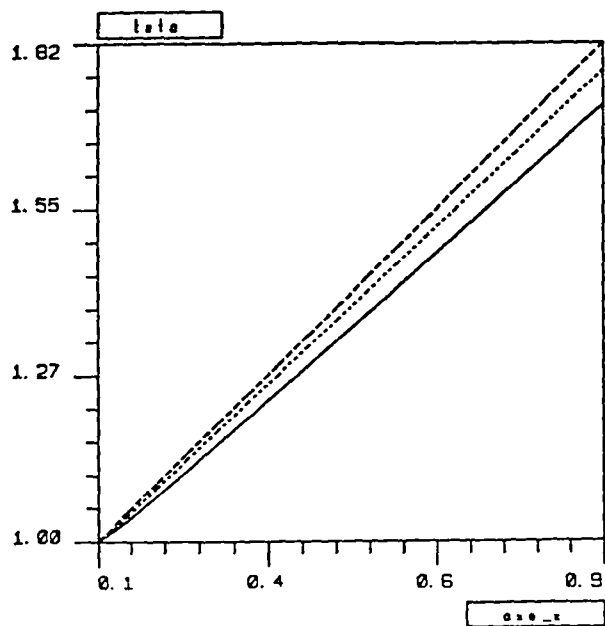
$$\theta = \theta_0 + (c_2 - 1)x$$

$$k = k_0 \left( \frac{\theta_0}{\theta_0 + (c_2 - 1)x} \right)^{\frac{1}{c_2 - 1}}$$

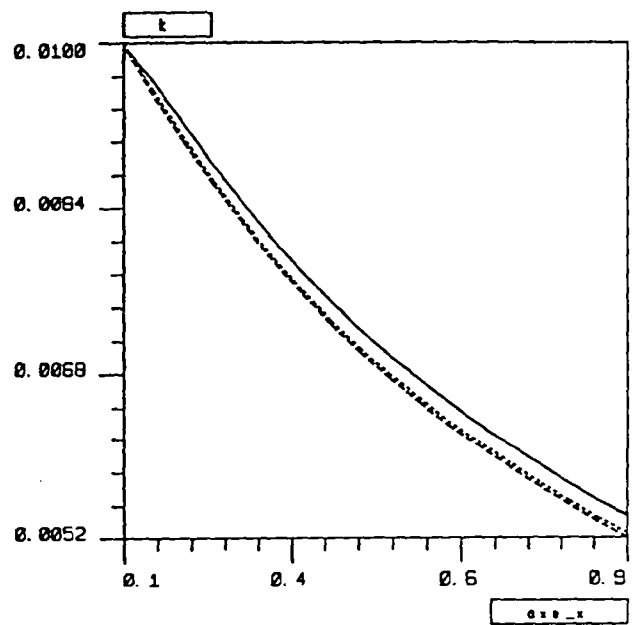
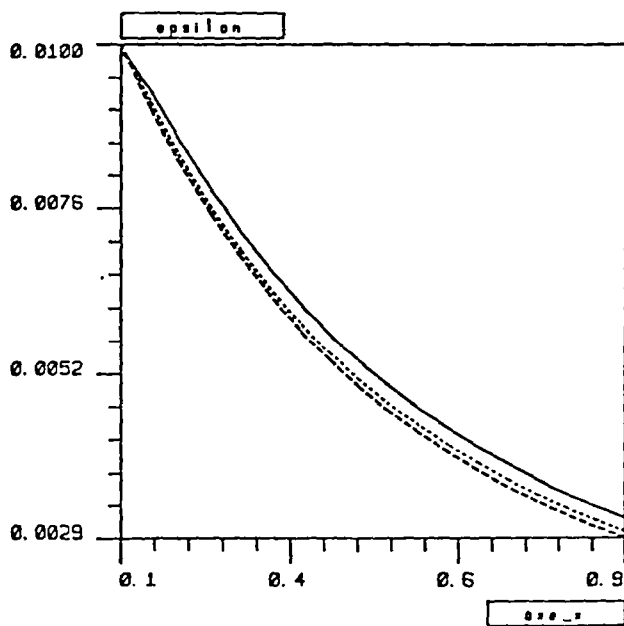
$$\varepsilon = \varepsilon_0 \left( \frac{\theta_0}{\theta_0 + (c_2 - 1)x} \right)^{\frac{c_2}{c_2 - 1}}$$

Hence, one can check the quality of the integration of the source terms along the characteristics curvs. The following figures show that the integration in  $\phi, \theta$  is more precise than the simple  $k, \varepsilon$  approach. It seems that it is because the  $k, \varepsilon$  model converges slower than the mixed model.

Behaviour of  $\theta$ ,  $k$  and  $\varepsilon$  versus the distance from the origine.



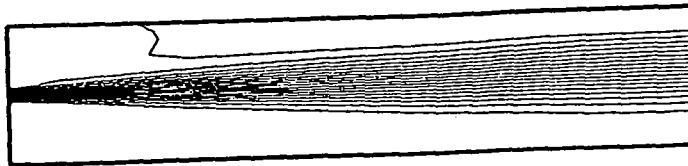
— :  $\epsilon$   
 - - - :  $\phi$   
 . . . :  $\theta$



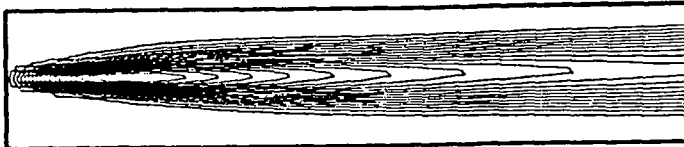
### *Free Shear Flow*

The objective of this test case is to check the behaviour of the model and of the code in high Reynolds number situations. This almost incompressible test case consist of a parallel flow with  $(u = 1, v = 0)$  if  $y \geq 0$  and  $(u = 2, v = 0)$  elsewhere. The computation is made at  $Re = 10^6$ . The absence of any solid boundary avoid the necessity of a low Reynolds modelling. We want a linear expansion for the width of the mixing layer zone. The initial and inflow profils of the turbulent quantities are given by the assumption that the flow is fully turbulent. This mean that the origine of the flow is placed before the computational domaine. So we take into account the velocity discontinuity through a few grid points and a pic is given for  $k$  and  $\epsilon$  at the same location. These profils are taken as inlet boundary conditions during the computation. For both symmetry and outlet boundary, Neumann boundary condition is applied for  $k$  and  $\epsilon$ . Furthermore, a Dirichlet boundary condition is applied on the pressure at the outlet boundary. The mesh has 600 nodes and 1200 triangles.

Contours for the mach number  $M = \frac{|u|}{\sqrt{\frac{p}{\rho}}}$  (top fig.), the turbulent kinetic energy and the rate of the eddy viscosity to the laminar one  $R = \frac{\mu_{turb}}{\mu_{lam}}$  computed with the  $k, \epsilon$  model. A linear expansion is predicted for the width of the mixing layer zone.



INCONNUE : 1 MNERO :VN	
20	0.2013
19	0.1956
18	0.1900
17	0.1843
16	0.1787
15	0.1730
14	0.1674
13	0.1617
12	0.1561
11	0.1504
10	0.1448
9	0.1391
8	0.1335
7	0.1278
6	0.1222
5	0.1165
4	0.1109
3	0.1052
2	0.9957E-01
1	0.9392E-01

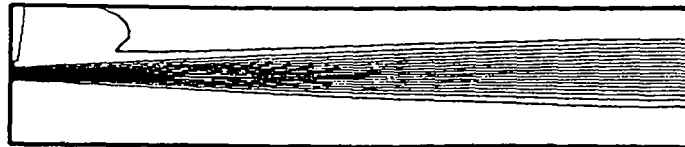


INCONNUE : 1 MNERO :VN	
20	0.5641E-01
19	0.5344E-01
18	0.5048E-01
17	0.4752E-01
16	0.4455E-01
15	0.4159E-01
14	0.3863E-01
13	0.3566E-01
12	0.3270E-01
11	0.2973E-01
10	0.2677E-01
9	0.2381E-01
8	0.2084E-01
7	0.1788E-01
6	0.1491E-01
5	0.1195E-01
4	0.8987E-02
3	0.6023E-02
2	0.3059E-02
1	0.9562E-04



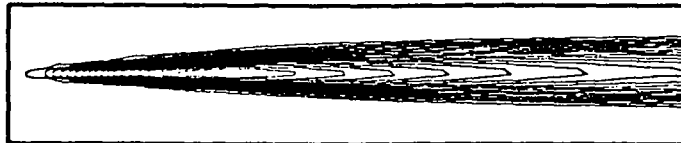
INCONNUE : 1 MNERO :VN	
20	1258.
19	1193.
18	1127.
17	1062.
16	996.9
15	931.6
14	866.4
13	801.1
12	735.8
11	670.5
10	605.2
9	539.9
8	474.6
7	409.4
6	344.1
5	278.8
4	213.5
3	148.2
2	82.94
1	17.65

The same contours computed with the mixed model.



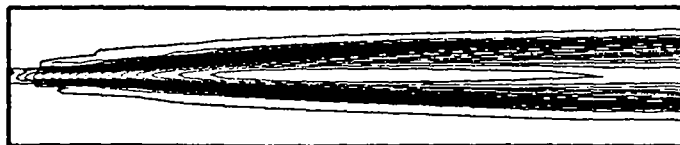
INCONNUE : 1 MNEHO :VN

20	0.2011
19	0.1955
18	0.1899
17	0.1843
16	0.1787
15	0.1731
14	0.1675
13	0.1619
12	0.1563
11	0.1507
10	0.1451
9	0.1395
8	0.1339
7	0.1283
6	0.1227
5	0.1171
4	0.1115
3	0.1059
2	0.1003
1	0.9475E-01



INCONNUE : 1 MNEHO :VN

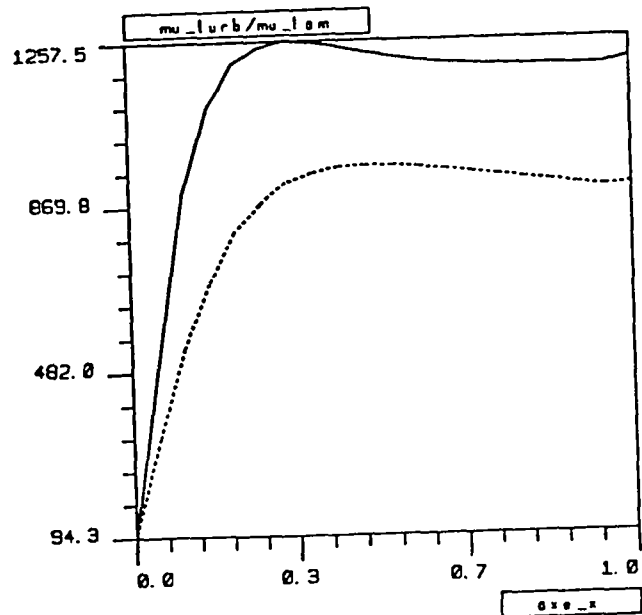
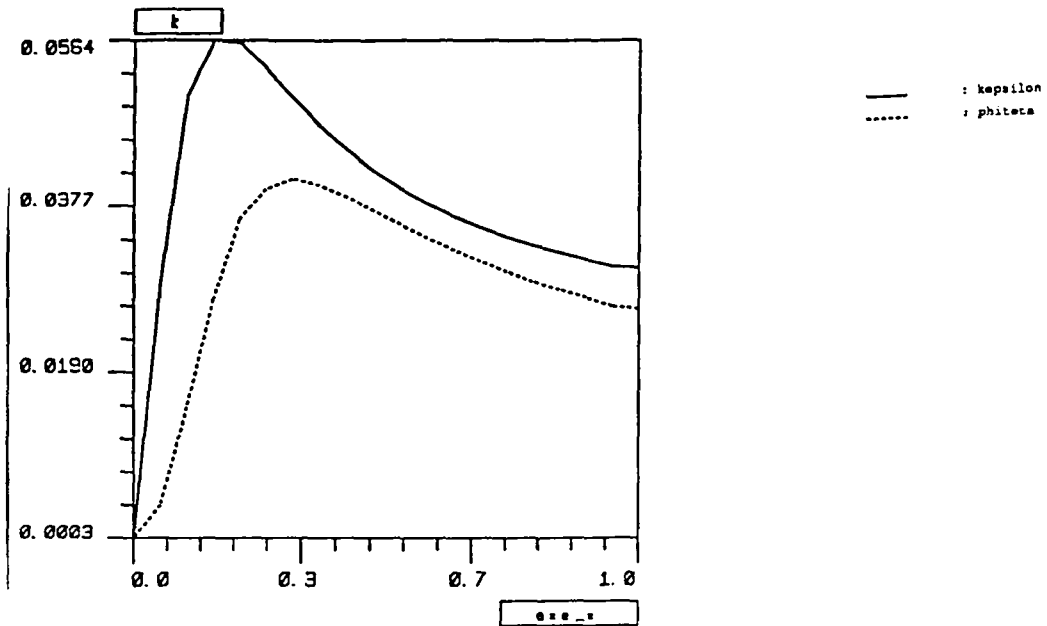
20	0.4098E-01
19	0.3883E-01
18	0.3667E-01
17	0.3451E-01
16	0.3236E-01
15	0.3020E-01
14	0.2804E-01
13	0.2589E-01
12	0.2373E-01
11	0.2157E-01
10	0.1942E-01
9	0.1726E-01
8	0.1510E-01
7	0.1295E-01
6	0.1079E-01
5	0.8634E-02
4	0.6478E-02
3	0.4321E-02
2	0.2165E-02
1	0.8700E-05



INCONNUE : 1 MNEHO :VN

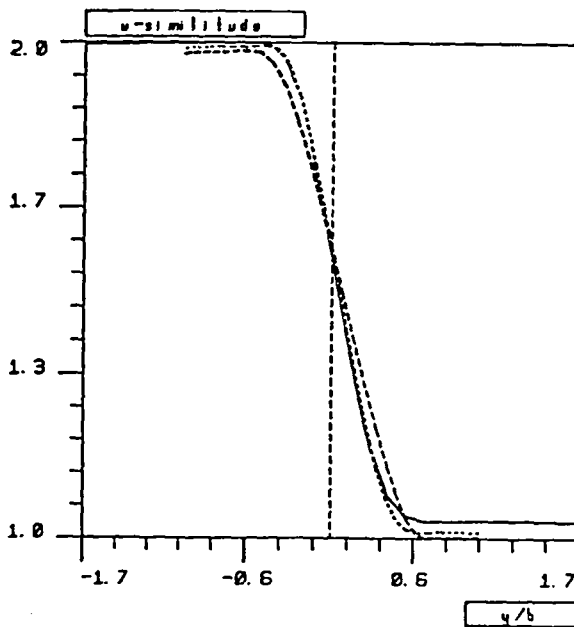
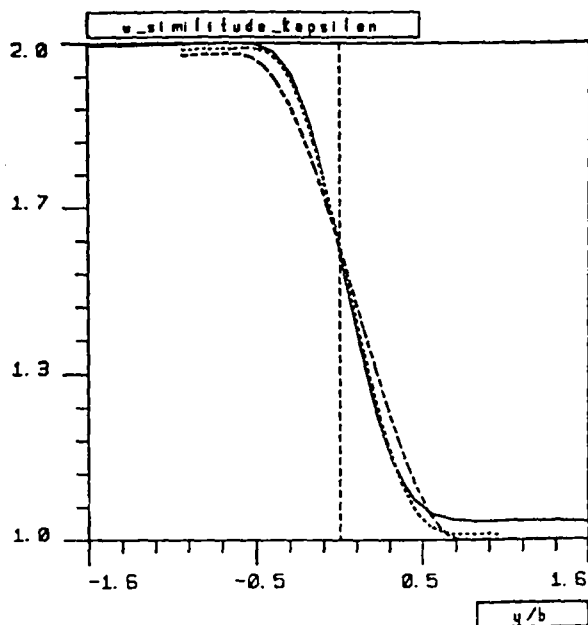
20	964.6
19	913.9
18	863.2
17	812.5
16	761.9
15	711.2
14	660.5
13	609.8
12	559.1
11	508.5
10	457.8
9	407.1
8	356.4
7	305.7
6	255.1
5	204.4
4	153.7
3	103.0
2	52.32
1	1.643

Behaviour of  $k$  (top) and  $\frac{\mu_{turb}}{\mu_{lam}}$  on the  $y = 0$  axis computed using the  $k, \epsilon$  and the mixed model.

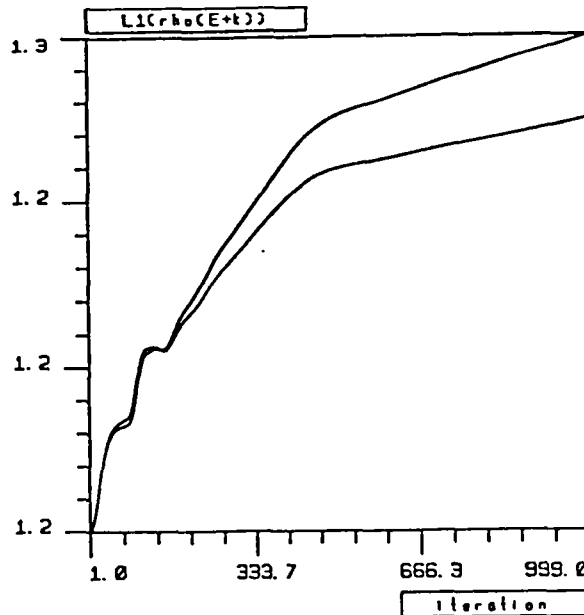
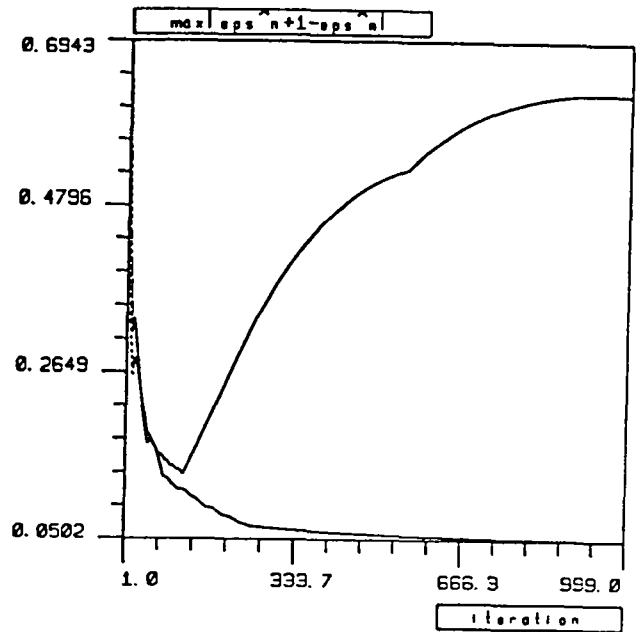
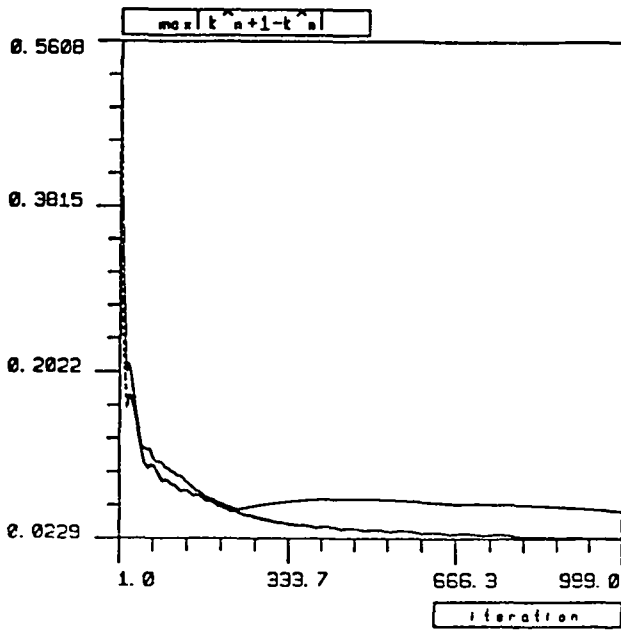




Similarity curves ( $u$  versus  $y/b$  with  $b$  the half width of the mixing layer) computed by  $k, \epsilon$  (top) and the mixed model.



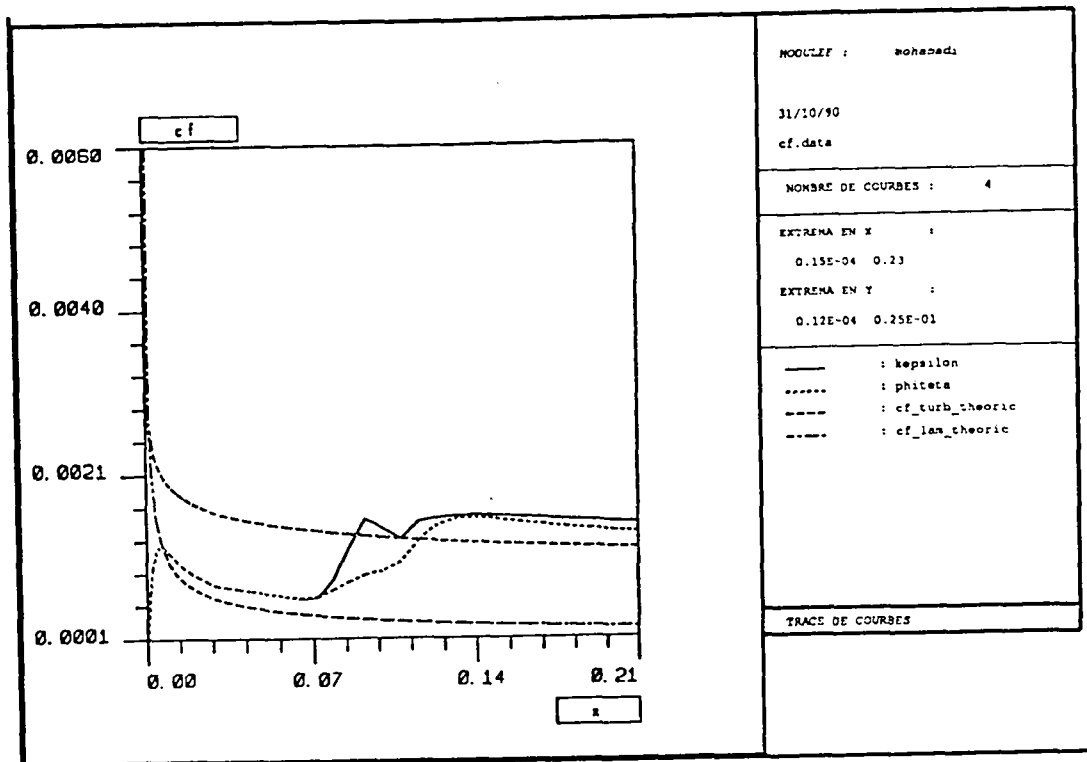
Convergence history of  $k$  (top),  $\varepsilon$  and the total energy  $E_t$  based on  $\max(\frac{k^{n+1}-k^n}{k^n})$ ,  $\max(\frac{\varepsilon^{n+1}-\varepsilon^n}{\varepsilon^n})$  and  $\int_{\Omega} \rho(\frac{u^2+v^2}{2} + k)$  computed by the  $k, \varepsilon$  (top curves) and the mixed model.



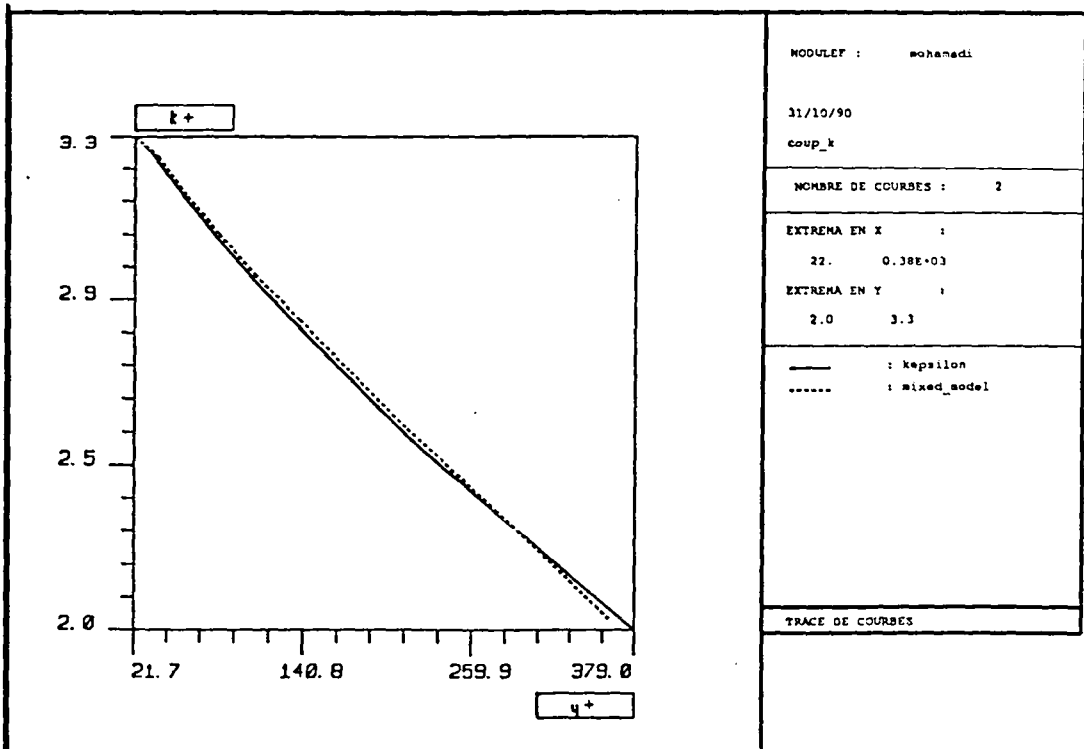
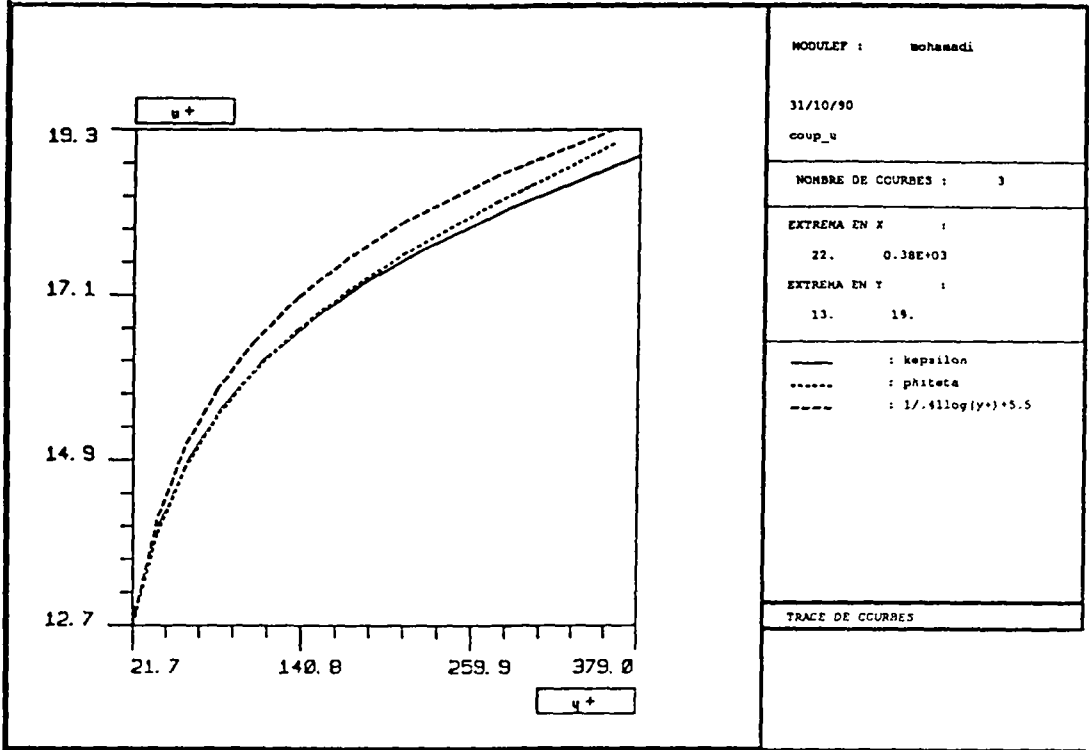
### Adiabatic Flate Plate

In the adiabatic case  $\frac{\partial T}{\partial n} = 0$ , the normal variation of the density close to the wall vanishes ( $\frac{\partial \rho}{\partial n} = 0$ ) this reduces (II.2.B) to its incompressible version. The initial and inlet levels of  $k$  and  $\epsilon$  are taken from  $k = au_\infty^2$  with  $a = 0.001$  and  $\epsilon = c_\mu \rho \frac{k^2}{\mu}$ . The mesh has 1500 nodes and 2842 triangles; the first node is placed at  $y = 3 \cdot 10^{-5}$  and the boundary of the computational domain at  $\delta = 5 \cdot 10^{-5}$  away from the wall; the plate has a length of 0.25. The computation is done for  $Re = 4 \cdot 10^7$  and  $M = 5$ . We make the assumption that the transition from laminar to turbulent is done between  $x = 0.08$  and  $x = 1.1$ .

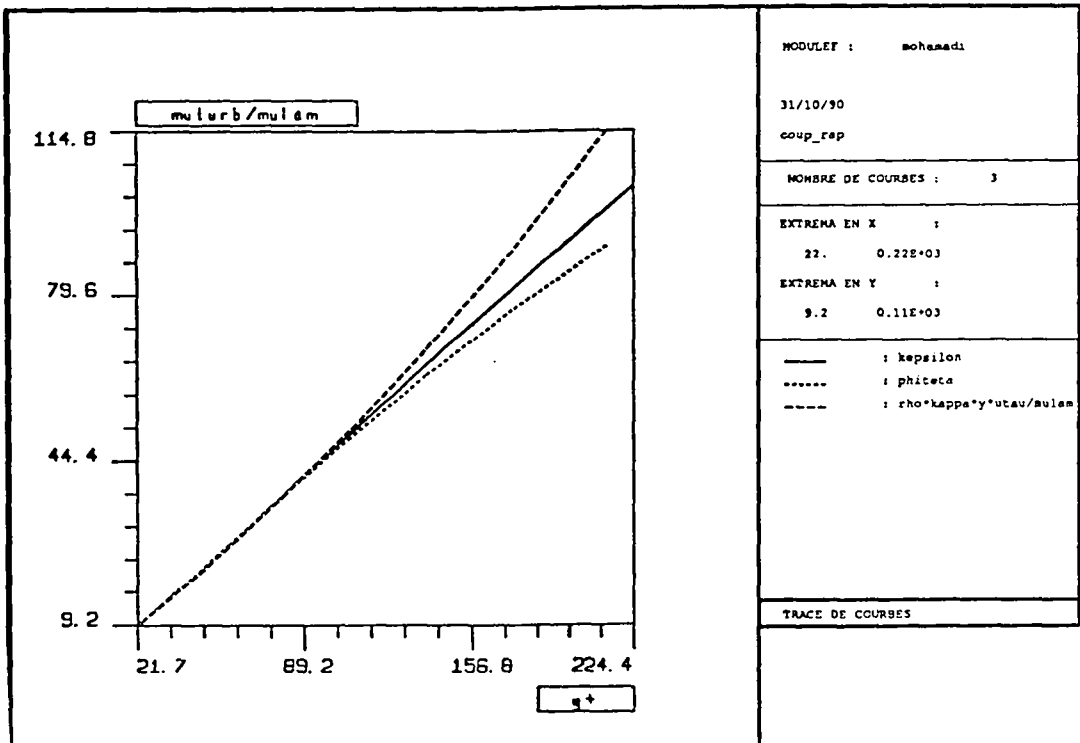
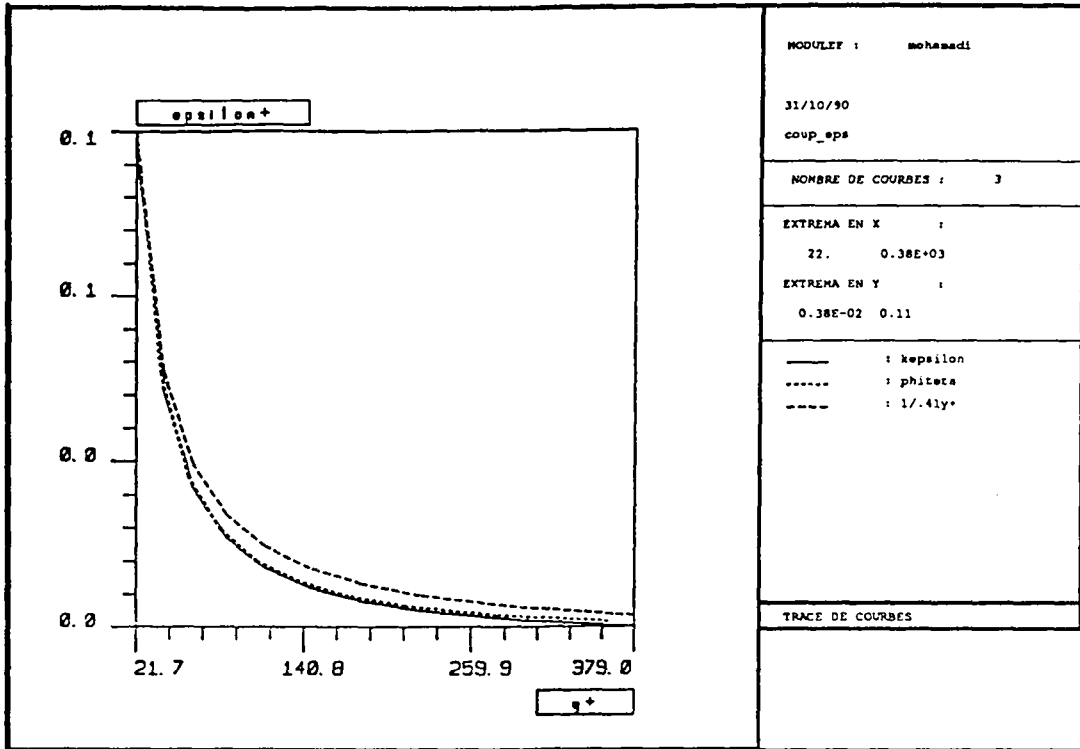
The friction coefficient ( $c_f = \frac{\tau_w}{0.5 \rho_\infty u_\infty^2}$ ) is compared to its laminar and turbulent theoretical expressions  $c_{f_{lam}} = 0.664 Re_x^{-1/2} f_{lam}$  and  $c_{f_{turb}} = 0.0368 Re_x^{-1/6} f_{turb}$  where  $f_{lam} = 0.950$  and  $f_{turb} = 0.449$  are compressible correction factors [COU1]. One can see that the  $c_f$  is overpredicted by both of the models. The mixed approach improves slightly the results.



Profiles of  $u^+ = \frac{u}{u_r}$  (top curves) and  $k^+ = \frac{k}{u_r^2}$  at  $x = 0.2$  computed with the two approach. The  $u^+$  profil is compared to  $u^+ = (1/41)\log(y^+) + 5.5$ .



Profils of  $\varepsilon^+ = \frac{\varepsilon \rho}{\mu u_\tau}$  (top curves) and  $R = \frac{\mu_1}{\mu_i}$ . These profils are compared to  $\varepsilon^+ = \frac{1}{\kappa y^+}$  and  $R = \rho u_\tau y / \mu$ .



## Conclusion

A two equations  $k, \varepsilon$  turbulence model has been introduced to a Navier-Stokes solver using characteristics and finite element method.

Furthermore, a new algorithm is proposed for the treatment of the convective part of the turbulent equations. In this algorithm the transport part of the equations are integrated with the source terms along the characteristics curves after a change of variables.

This new algorithm is interesting from the point of view of numerical analysis because it has high stability. Furthermore, such an approach proves that the coupled system ( $k - \varepsilon$ ), and not each equation individually, can be stable.

At this time, we are unable to consider flows including separation because of the use of wall laws. To avoid this difficulty, following Patel [PA2] we are going to introduce a two-layer approach ; the  $\varphi, \theta$  model for the high Reynolds number situations and a  $k, L$  low Reynolds model or an algebraic Baldwin-Lomax eddy viscosity model including Goldberg modification for the near wall regions.

## V. References :

- [AN1] F. Angrand, J. Erhel, "Simulation par éléments finis d'écoulements compressibles sur calculateurs vectoriels", INRIA Report 622.
- [AH1] B. Ahmadi-Befrui. Assessment of variants of  $k, \varepsilon$  model for engine flow applications. IJNMF Vol. 9, 1986.
- [BE1] J.P. Benqué, O. Daubert, J. Goussebaile, H. Hauguel : Splitting up techniques for computations of industrial flows. In *Vistas in applied mathematics*, A.V. Baladrishnan ad. Optimization Software inc. Springer, 1986.
- [PI1] O. Pironneau, On the transport-diffusion algorithm and its applications to the Navier-Stokes equations. *Numer. Math.* 38, 309-332, 1982.
- [PI2] O. Pironneau, *Finite Element Methods for Fluids*, Masson, 1989.
- [RA1] P.A. Raviart, "Cours de DEA d'Analyse Numérique Paris 6", 1989.
- [RO1] P. Rostand, Sur une méthode de volumes finis en maillage non structuré pour le calcul d'écoulements visqueux compressibles. Thesis, Université Paris VI, 1989.
- [CA1] B. Cardot, Modélisation de la turbulence par des méthodes de type  $k, \varepsilon$  et homogénéisation. Thesis, Université Paris VI, 1989.
- [CA1] B. Cardot, B. Mohammadi, O. Pironneau, A Few tools for the implementation of turbulence models in Navier-Stokes solvers. To appear.

opolis, April 1990.

odel, To appear.

- [BO1] S. Boivin, INRIA Report num. 923.
- [CH1] T. Chacon, O. Pironneau : On the mathematical foundations of the  $k - \varepsilon$  model. In *Vistas in applied mathematics*. A.V. Balakrishnan ed. Optimization Software inc. Springer, 1986.
- [CO1] T.J. Coakley, Turbulence modeling methods for the compressible Navier-Stokes equations. AIAA-83-1693.
- [COU1] J. Cousteix : *Turbulence et couche limite*, cepadues editions 1990.

- [DO1] J. Douglas, T.F. Russel : Numerical methods for convection dominated diffusion problems bases on combining the method of characteristics with finite element method or finite differences method. *SIAM J. Numerical analysis*, 19, 5 871-885, 1982.
- [LS1] B.E. Launder, D.B. Spalding : *Mathematical models of turbulence*. Academic Press, 1972.
- [ST1] B. Stoufflet, L. Fezoui, A class of implicit upwind schemes for Euler simulations with unstructured meshes, to appear in *Journal of Computational Physics*.
- [ST2] B. Stoufflet, Thesis University of Paris VI, 1984.
- [VI1] P.L. Viollet : On the modelling of turbulent heat and mass transfers for computations of buoyancy affected flows. *Proc. Int. Conf. Num. Meth. for Laminar and Turbulent Flows*. Venizia, 1981.
- [VA1] D. Vandromme, Contribution à la modélisation et la prédiction d'écoulements turbulents à masse volumique variable. Thesis, University of Lille (1983).
- [GR1] F. Grasso, C. Speziale Supersonic flow computations by two-equation turbulence modeling. *AIAA 89-1951*.
- [PA1] V.C. Patel, W. Rodi, G. Scheuerer : Turbulence models for near-wall and low Reynolds number flows : a review *AIAA J* Vol. 23, no 9.
- [PA2] V.C. Patel, H.C. Chen, Near-wall turbulence models for complex flows including separation. *AIAA Journal* vol. 29, no. 6, June 1988.
- [GE1] M. Jaeger, Simulation numérique d'écoulements turbulents incompressibles et isothermes de fluides newtoniens par éléments finis tridimensionnels. Thesis Univ. Tech. Compiègne (1990).
- [WU1] C.T. Wu, J. H. Ferziger and D.R. Chapman, Simulation and modelling of homogeneous compressed turbulence, Dept. of mechanical engineering Stanford Univ. 1985.
- [ZI1] O.C. Zienkiewicz, *The finite element method in engineering science*. Mac Graw Hill 1977.



## APPENDIX A - The Navier-Stokes Solver

We give now a summary description of the Navier-Stokes solver, more details could be found in [PI2] and [RO1]. The conservative NSE are

$$\frac{\partial W}{\partial t} + \nabla \cdot (F(W) - N(W)) = 0 \quad (NS)$$

where  $W = (\rho, \rho u, \rho v, \rho E)$  is the vector of conservative variables,  $F$  the convective operator and  $N$  the diffusive one. Let  $\Omega_h = \cup_j T_j$  a discretization by triangles of the computational domain  $\Omega$  and let  $\Omega_h = \cup_i C_i$  its partition in cells building for a node  $s_i$  by taking the medians, not originating from  $s_i$  of the triangle surrounding it. Thus, we could associate to each  $w_h \in V_h$  a continuous  $P^1$  function on our triangulation, a  $w'_h$  piecewise constant function on cells by

$$w'_h|_{C_i} = \frac{1}{|C_i|} \int_{C_i} w_h$$

conversely, knowing  $w'_h$  piecewise constant,  $w_h$  is obtained as  $w_h(S_i) = w'_h|_{C_i}$ . If we suppose that  $F$  vary linearly on each triangle, the classical weak formulation of NS involving  $V_h$  : Find  $W_h \in (V_h)^4$  such that  $\forall \phi_h \in V_h$

$$\int_{\Omega} \frac{\partial W_h}{\partial t} \phi_h - \int_{\Omega} (F - N)(W_h) \nabla(\phi_h) + \int_{\partial\Omega} (F - N) \cdot n \phi_h = 0 \quad (P)$$

is equivalent to its Petrov-Galerkin weak formulation obtained by taking in the convective part of  $P$  for  $\phi_h$  the characteristic function of  $C_i$ . Hence, after an explicite time integration we have for all nodes  $s_i$  :

$$|C_i| \left( \frac{W^{n+1} - W_i^n}{\Delta t} \right) + \int_{\partial C_i} F_d(W^n) \cdot n = R.H.S.$$

for  $R.H.S. = - \int_{\Omega_h} N(W^n) \nabla(\phi_h) + \int_{\partial\Omega} N(W^n) \cdot n \phi_h$  we use a centred scheme.  $F_d(W_h^n) = F(W_{\partial\Omega})$  on  $\partial C_i \cap \partial\Omega$  and elsewhere  $F_d$  is a piecewise constant approximation of  $F(W)$  verifying

$$\int_{\partial C_i} F_d \cdot n = \sum_{j \neq i} \Phi(W'|_{C_i}, W'|_{C_j}) \int_{\partial C_i \cap C_j} n$$

writing  $B$  the jacobian of  $F$ , we take for  $\Phi$  the Osher proposition  $\phi_{Osher} = \frac{1}{2}(F(u) + F(v) - \int_v^u |B(w)| dw)$ , where the integral is evaluated along a path piecewise parallel to characteristics. Spatial second order accuracy is obtained by the use of a MUSCL like extension using upwinded gradients.

Such an explicit scheme gives slow convergence to a steady state because we are limited by a CFL of order 1. In order to avoid this restrictive condition, we use a linearly implicit scheme

$$M(W^n)\delta W^{n+1} = b \quad (E)$$

where  $\delta W^{n+1} = W^{n+1} - W^n$ ,  $b = -\int_{\partial C} (F_d - N)(W^n) \cdot n$  is the physical flux through  $\partial C$  and  $M = \frac{\Delta t}{|C|}I + \frac{\partial(F_d - N)}{\partial W}(W^n)$ .

The boundary conditions are taken into account in the matrix and in the right hand side of  $E$  as described in [ST1], [ST2], [RO1].

*APPENDIX B - Some necessary conditions for the well posedness of the NS with wall laws*

In this paragraph, the viscosity and the thermal conductivity are taken as constant.

Let us check that the NS equations with the boundary conditions (B.1) at the solid wall  $\partial\Omega_w$  are somehow well posed. A similar analysis is available in [RO1] for the NS equations with slip boundary conditions.

$$\begin{aligned} u \cdot n &= 0 \\ n \cdot N \cdot \tau &= -\rho u_\tau^2 \\ u \cdot N \cdot \tau + \kappa \frac{\partial T}{\partial n} &= -\rho u_\tau^2 + T_\tau u_\tau \end{aligned}$$

where  $n$  is the outward normal,  $\tau$  the tangential vector to the wall in the flow direction and  $N = \frac{1}{Re}(\nabla u + \nabla u^T - \frac{2}{3}(\nabla \cdot u)I)$  is the viscous tensor.

First, such a set of boundary conditions guaranties the decrease of the energy and entropy if  $\rho u \cdot \tau \leq \frac{T_\tau}{u_\tau}$ ; indeed using the divergence formula on (II.1.3) :

$$\frac{d \int_\Omega E}{dt} = - \int_{\partial\Omega} ((E+p)(u \cdot n) + \int_{\partial\Omega} (u \cdot N(u) \cdot n + \kappa \frac{\partial T}{\partial n})$$

Away from the wall, we take  $N(u) = 0$ ,  $\frac{\partial T}{\partial n} = 0$  and  $(E+p)(u \cdot n) = \text{constant}$  on  $\partial\Omega_\infty$ , so

$$\frac{d \int_\Omega E}{dt} = - \int_{\partial\Omega_w} -\rho u_\tau^2 (u \cdot \tau) + u_\tau T_\tau$$

Notice that on an adiabatic wall ( $\frac{dT}{dn} = 0$ ), the decay of energy is always guaranteed. But if we are interested in an isothermic wall, only  $\frac{\partial T}{\partial n} < 0$  (i.e. cold wall) guarantees the decay of energy. The entropy  $\rho s = \rho \log(\frac{\rho^{\gamma-1}}{T})$  equation is obtained from the NS equation :

$$\frac{\partial \rho s}{\partial t} + \nabla \cdot (\rho u s) = -\frac{1}{T}(\kappa \Delta T + F)$$

with  $F = \mu(\frac{1}{2}(|\nabla u + \nabla u^t|^2 - \frac{2}{3}(\nabla \cdot u)^2) \leq 0$ . Now, using Green and divergence formulas, for the entropy we have :

$$\frac{d \int_\Omega \rho s}{dt} = - \int_\Omega (\frac{F}{T} + \kappa \frac{|\nabla T|^2}{T^2}) - \int_{\partial\Omega_w} \frac{\kappa}{T} \frac{\partial T}{\partial n}$$

because  $\rho s(u \cdot n) = \text{constant}$ ,  $N = 0$ , and  $\nabla T = 0$  on  $\partial\Omega_\infty$ .

**ISSN 0249 - 6399**